

SPECTRAL DEPENDENCE OF THE BROAD EMISSION-LINE REGION IN AGN

A. Wandel

Racah Institute of Physics, The Hebrew University of Jerusalem 91904, Israel

Abstract.

We derive a theoretical relation between R_{BLR} , the size of the broad-emission-line region of active galactic nuclei, and the observed soft X-ray luminosity and spectrum. We find that in addition to the well known $R_{BLR} \sim L^{1/2}$ scaling, R_{BLR} depends also on the soft X-ray spectral slope. Applying this relation to calculate a predicted BLR radius and emission-line width, we show that including the dependence on the spectrum significantly improves the agreement between the calculated BLR radius and the radius independently determined from reverberation mapping as well as the the agreement between the calculated velocity dispersion and the observed FWHM of the $H\beta$ line. We evaluate a theoretical expression for the line width, providing a physical explanation to the anti-correlation between the soft X-ray slope and the emission-line width observed in narrow-line Seyfert galaxies.

1. Introduction

Recent results from reverberation-mapping of the broad emission-line regions (BLR) in AGNs indicate that the BLR distance from the central radiation source roughly scales as $r \propto L^{1/2}$ (Koratkar & Gaskell 1991; Kaspi et.al. 1996). Our model provides a physical explanation to this scaling, and predicts an additional testable dependence on the spectral shape.

Most workers today agree that the line width in AGN is induced by Keplerian bulk motions. If this is the case, the BLR distance is directly related to the line width. A particularly interesting group in this respect are Narrow-Line Seyfert Galaxies (NLS1), which have narrower emission lines than ordinary Seyfert 1 galaxies, and often show steep soft X-ray spectra. In mixed samples (NLS1 and ordinary AGN) the soft X-ray spectral index is anticorrelated with the $H\beta$ line width and with the $H\beta$ equivalent width. (Boller, Brandt, & Fink 1996; Wang, Brinkmann and Bergeron 1996, hereafter WBB).

We derive simple analytic relations between soft X-ray continuum spectrum (luminosity and spectral index) and the BLR size and the width of the broad emission lines, explaining the observed anticorrelation between the X-ray slope and the line width and equivalent width (Wandel 1997; Wandel and Boller 1998). Application of this model to samples of AGN gives a good agreement with the BLR sizes determined by reverberation mapping, and with the observed FWHM($H\beta$).

2. The Model

While there is probably a range of physical conditions (ionization parameter and density etc.) in the broad H β line-emitting gas in AGNs, the emission of each line is dominated by emission in a relatively narrow optimum range of conditions (Baldwin et al. 1995). We will therefore make the assumption that the conditions relevant for H β can be approximated by a single value. We show that within the observational constraints on the far UV and soft X-ray bands of AGN spectra, the BLR size and the line width predicted by the model are not very sensitive to the detailed shape of the spectrum in the EUV band. We then estimate the BLR size, and assuming Keplerian velocity dispersion we relate it to the line width. The new element in our scheme is the use of the soft X-ray spectral index and luminosity to estimate the ionizing spectrum. The spectral index enters in the model as follows: a softer (that is steeper) spectrum has a stronger ionizing power, and hence the BLR is formed at a larger distance from the central source, has a smaller velocity dispersion and produces narrower emission lines. We parameterize the form of the ionizing EUV continuum in terms of the the break between the UV and X-ray bands and the measured soft X-ray slope α_x .

2.1. The BLR radius

We assume that the spatial extent of the BLR may be represented by a characteristic size - e.g. the radius at which the emission peaks. The physical conditions in the line-emitting gas are largely determined by the ionization parameter (the ratio of ionizing photon density to the electron density, n_e , e.g. Netzer, 1990) $U = Q_{ion}/4\pi R^2 c n_e$ where the ionizing photon flux (number of ionizing photons per unit time) is $Q_{ion} = \int_{E_0}^{\infty} F(E) \frac{dE}{E}$, $F(E)$ is the luminosity per unit energy, and $E_0 = 1$ Rydberg=13.6 eV. Defining the ionizing luminosity, $L_{ion} = \int_{E_0}^{\infty} F(E) dE$ and the mean energy of an ionizing photon, $\bar{E}_{ion} \equiv L_{ion}/Q_{ion}$, the BLR radius may be written as

$$R = \left(\frac{L_{ion}}{4\pi c \bar{E}_{ion} U n_e} \right)^{1/2} = 13.4 \left(\frac{L_{x44}}{U n_{10} \epsilon_x} \right)^{1/2} \text{ light-days} \quad (1)$$

where $n_{10} = n_e/10^{10} \text{ cm}^{-3}$, $L_{x44} = L_x/10^{44} \text{ erg s}^{-1}$ is the observed X-ray luminosity, $\epsilon = \bar{E}_{ion}/E_0$ is the mean photon energy in Rydberg, and $\epsilon_x = \epsilon L_x/L_{ion} = L_x/E_0 Q_{ion}$. Typical values in the gas emitting the high excitation broad lines are $U \sim 0.1 - 1$ and $n_e \sim 10^{10} - 10^{11} \text{ cm}^{-3}$ (e.g. Rees, Netzer and Ferland, 1989), so that $U n_{10} \sim 0.1 - 10$.

The ionizing flux is dominated by the EUV continuum in the 1-10 Rydberg regime, where most of the ionizing photons are emitted. Since the the continuum in this range cannot be observed directly, we try to estimate it by extrapolation from the nearest observable energy bands. The far UV spectrum has been observed beyond the Lyman limit, for about 100 quasars (Zheng et al, 1996), to wavelengths of 600 Å, and for a handful luminous, high redshift quasars to wavelengths of 350 Å. The average spectrum has a slope of $\alpha \sim 1$ in the 1000–2000 Å band, and below 900 Å it steepens to $\alpha \sim 2$. We assume that the soft X-ray spectrum can be extrapolated to lower energies down to some break

energy E_b , and below the break we take E^{-2} . For the hard X-rays ($E > 2$ keV) we use the “universal” $E^{-0.7}$ power law, observed in most AGN with a high energy cutoff at 100 keV.

2.2. Line width

Assuming that the line width is induced by Keplerian motion in the gravitational potential of the central mass, the velocity dispersion corresponding to the full width at half maximum of the emission lines is given by $v \approx \sqrt{GM/R}$ where M is the mass of the central black hole and r the distance of the broad line region from the central source. Equation (1) gives

$$v \approx 1900 \left(\frac{Un_{10}\epsilon_x}{L_{x44}} \right)^{1/4} \left(\frac{M}{10^7 M_\odot} \right)^{1/2} \text{ km s}^{-1}. \quad (3)$$

In order to relate the unknown mass to the observed luminosity we assume that the central mass approximately scales with the luminosity (Dibai 1981; Joly et al. 1985; Wandel & Yahil 1985; Wandel & Mushotzky 1986). In terms of the Eddington ratio these authors find for large AGN samples $L/L_{Edd} \approx 0.01 - 0.1$. Within this distribution, bright objects tend to have slightly larger L/M ratios than faint ones (cf. Koratkar and Gaskell 1991) roughly $L/M \propto L^{1/4}$ or $M \propto L^{3/4}$. Combining this with the correlation between the optical and the X-ray luminosities $L_x \propto L_{opt}^{0.75 \pm 0.05}$ (Kriss 1988; Mushotzky and Wandel 1989) gives

$$M \approx 7 \times 10^7 L_{x44} \left(\frac{L/L_{Edd}}{0.01} \right)^{-1} M_\odot. \quad (4)$$

and with eqs. (2) and (3) the line-width may be related directly to the observed X-ray luminosity and spectral index:

$$v(FWHM) \approx 5000 \eta \epsilon_x^{1/4} (\alpha_x) L_{x44}^{1/4} \text{ km s}^{-1} \quad (5)$$

where $\eta \equiv (Un_{10})^{1/4} (L/L_{Edd}/0.01)^{-1/2}$ combines all the unknown parameters; for the $Un_{10} \sim 0.1 - 10$ and $L/L_{Edd} \sim 0.01 - 0.1$ stated above we have $\eta \sim 0.2 - 2$.

3. Comparison With The Data

3.1. BLR radius

We have Compared the BLR size calculated from the model with the distance from the central source obtained by reverberation mapping of the H β line, for a sample of 10 AGN for which reverberation and X-ray data were available (Figure 2). As we discuss below, the agreement *actually improves* by taking the X-ray spectral slope into account.

In the model calculations we have used the spectral index from the power-law fit to the ROSAT 0.1-2.4 keV band and $E_b = 1$ Ryd, The horizontal error bars represent the combined error in the luminosity and in the spectral index. Allowing for the uncertainty in $Un_{10} \sim 0.1 - 1$ (represented by the dashed lines in Figure 1), the agreement is quite good: all the points lie well within these boundaries.

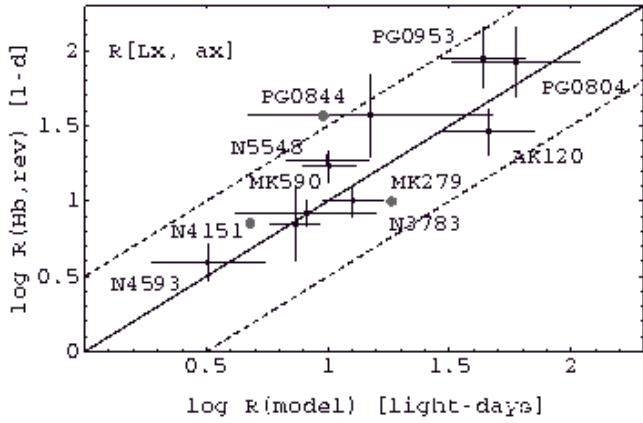


Figure 1. The BLR size determined from reverberation mapping of the $H\beta$ line vs. the radius calculated from the model using the observed X-ray luminosity and spectral index. (Wandel 1997). The grey circles represent the radius calculated from the model without taking the spectral dependence into account. The solid line represents $r_{rev} = r_{model}$ for $Un_{10} = 1$ while the dashed parallel lines above and below it correspond to $Un_{10} = 0.1$ and 10 respectively.

In order to test the significance of our model, we have calculated the BLR radii *without* taking into account the spectral dependence (that is, assuming all objects have *the same* soft X-ray spectral slope, which we set to the sample average, $\alpha_x = 1.45$). We find that the difference between the BLR size (calculated using only the luminosity scaling) and the reverberation size is significantly larger than the difference when the spectral dependence is taken into account for three objects (NGC 4151, PG 0844 and NGC 3783) shown as gray dots in Figure 1. Those are the objects with the most extreme values of α_x . For the other objects in the sample the difference is small in both calculations.

3.2. Line width-spectral index correlation

Equation (5) predicts an explicit relation between the velocity dispersion (associated with the line width), the X-ray luminosity and the spectral index, namely a surface in the $\alpha_x - v - L_x$ space. For a fixed value of L_x this gives a curve in the $v - \alpha_x$ plane. Figure 2 shows such curves of FWHM vs. α_x for several values of the luminosity, $L_x = 10^{42} - 10^{45} \text{ erg s}^{-1}$ (Wandel 1997). Overplotted are the data points - FWHM($H\beta$) vs. α_x for a sample of AGN (see below). The model seems to reproduce the distribution of the data very well, and in particular it explains the observed anticorrelation between the $H\beta$ line width and the soft X-ray spectral index and the lack of objects with broad lines and steep soft X-ray spectra.

3.3. Predicted vs. observed line width

In order to test the model prediction over the three dimensional $\alpha - v - L_x$ space we compare the observed line width to the value calculated with equation (5)

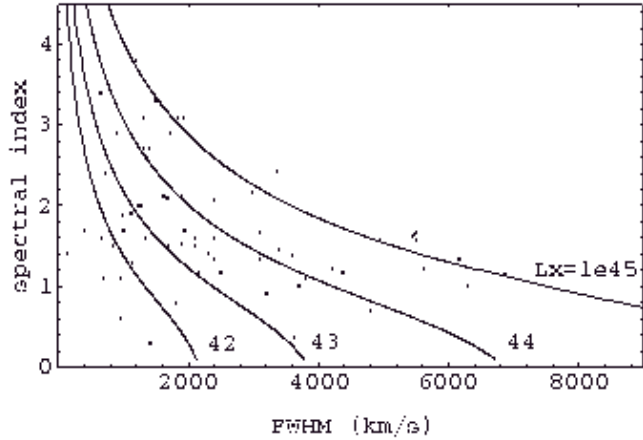


Figure 2. Theoretical curves of the X-ray spectral index vs. v (BLR) for fixed values of $L_x = 10^{42} \text{ erg s}^{-1}$ (lower curve) to $L_x = 10^{45} \text{ erg s}^{-1}$ (upper curve) superposed on the data for the sample of NLS1s and normal Seyferts.

using the measured X-ray spectral index and luminosity for a sample consisting of 33 ordinary AGN from Walter & Fink (1993) combined with 32 NLXGs (Boller, Brandt, & Fink 1996).

As can be seen in Figure 3, the agreement is very good, and most of the objects fall well within the uncertainty strip of $\log FWHM(\text{obs}) = \log v(\text{mod}) \pm 0.5$. When the spectral information is not taken into account the correlation is significantly weaker. The correlation coefficients between the observed and calculated line widths are $r = 0.533$ and 0.316 respectively.

4. Equivalent width

The data show that (WBB) AGN with a steep soft X-ray spectrum have a lower $EW(H\beta)$ than flat-spectrum AGN. We now show that also this anti-correlation of the $H\beta$ equivalent width and α_x follows in the framework of the model. To see this we recall that the equivalent width measures the fraction of the continuum flux reprocessed and emitted in the line. We have shown that the BLR distance from the central source increases with the soft X-ray spectral index. The two-zone photoionization analyses of the BLR (Brotherton et al. 1994) shows that the covering factor in the more extended part BLR part, the Intermediate Line Region is about 10% of that in the near BLR, indicating the integral covering factor decreases with radius. If such a geometry is common in AGN, a steeper (softer) ionizing spectrum will lead to a smaller covering factor. This implies that the equivalent width decreases with increasing (steepening) spectral index, as observed.

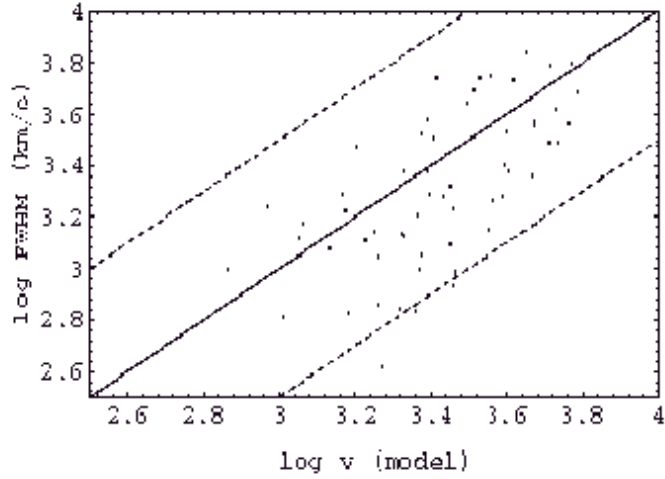


Figure 3. The observed FWHM(H β) vs. the v(BLR) calculated from the model using the observed L_x and spectral index. The diagonal line represents the equality ($v = FWHM$) for $\eta = 0.6$ (see equation [5]), while the dashed parallel lines above and below the diagonal are for $\eta = 0.2$ and 2 respectively.

References

Baldwin, J. A. et al. 1995, ApJ, 455, L118
 Boller, T., Brandt W. N., & Fink, H. 1996 A&A, 305, 53
 Brotherton M. S. et al. 1994, ApJ, 430 495
 Dibai, E. A. 1981, Soviet Astronomy Letters, 7, 248
 Kriss, G.A. 1988, ApJ, 324, 809
 Joly, M., Collin-Souffrin, S., Masnou, J.L., & Nottale, L. 1985, A&A, 152, 282
 Kaspi, Sh., Smith, P. S., Maoz, D., Netzer, H., & Jannuzi, T. J. 1996, ApJ, 471, L75
 Koratkar, A. P. & Gaskell, C. M. 1991, ApJ, 370, L61
 Mushotzky, R. F. & Wandel, A. 1989, ApJ, 339, 674
 Netzer, H. 1990 in Saas-Fee Advanced Course 20, "Active Galactic Nuclei", ed. T.J.-L. Courvoisier and M. Major (Berlin: Springer), p. 57
 Rees, M., Netzer H., Ferland, G.J. 1989. ApJ, 347, 640
 Walter, R. & Fink, H. H. 1993, A&A, 274, 105
 Wandel, A. 1997, ApJ430, 131
 Wandel, A. & Boller, Th. 1998, A&A, 331, 884
 Wandel, A. & Mushotzky, R. F. 1986, ApJ, 306, L61
 Wandel, A. & Yahil, A. 1985, ApJ, 295, L1
 Wang, T., Brinkmann, W., & Bergeron, J. 1996, A&A, 309, 81 (WBB)